

Catalysis Science & Technology

Accepted Manuscript



This is an *Accepted Manuscript*, which has been through the Royal Society of Chemistry peer review process and has been accepted for publication.

Accepted Manuscripts are published online shortly after acceptance, before technical editing, formatting and proof reading. Using this free service, authors can make their results available to the community, in citable form, before we publish the edited article. We will replace this *Accepted Manuscript* with the edited and formatted *Advance Article* as soon as it is available.

You can find more information about *Accepted Manuscripts* in the [Information for Authors](#).

Please note that technical editing may introduce minor changes to the text and/or graphics, which may alter content. The journal's standard [Terms & Conditions](#) and the [Ethical guidelines](#) still apply. In no event shall the Royal Society of Chemistry be held responsible for any errors or omissions in this *Accepted Manuscript* or any consequences arising from the use of any information it contains.

Theoretical study on the catalytic role of water in methanol steam reforming on PdZn(111)

Zheng-Qing Huang,^a Bo Long^b and Chun-Ran Chang^{*a}

^a School of Chemical Engineering and Technology, Xi'an Jiaotong University, Xi'an 710049, China

^b College of Information Engineering, Guizhou Minzu University, Guiyang 550025, China

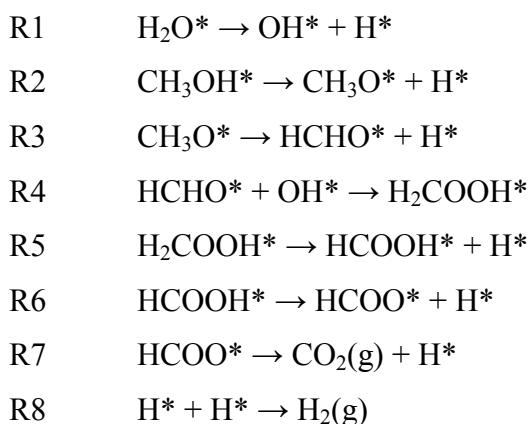
Abstract: Methanol steam reforming (MSR) is a promising method for large-scale production of hydrogen. While significant efforts have been devoted to the reaction mechanisms, the function of water except serving as a reactant is little known. Here we present a density functional study of the catalytic role of water in the whole MSR process on the PdZn(111) surface. It is shown that water not only influences the adsorption of reaction species but also the kinetics of the elementary steps of MSR. The calculated adsorption energies of reaction species including CH₃OH*, CH₃O*, H₂COOH*, HCOOH* and HCOO* increase by some 0.10–0.30 eV in the presence of co-adsorbed water. Importantly, water is found to substantially favor six dehydrogenation steps of MSR through lowering the activation barriers by 0.25–0.46 eV without being consumed, providing compelling evidence for the catalytic role of water in MSR. Depending on the manner in which water participates in the reactions, the catalytic mechanisms of water are classified into two categories, the solvation effect and the H-transfer effect. For the dehydrogenation steps involving O–H bond cleavage, both of the two mechanisms are applicable and show a slight difference in reducing the reaction barriers. However, for the dehydrogenation steps involving C–H bond cleavage, the catalytic function of water can only be realized through the solvation effect. These results uncover the catalytic role of water in MSR and are helpful for understanding the water effect in other chemical transformations.

1. Introduction

Methanol steam reforming ($\text{CH}_3\text{OH} + \text{H}_2\text{O} \rightarrow \text{CO}_2 + 3\text{H}_2$, MSR) is one of the most promising methods for on-demand hydrogen production because of the advantageous properties of methanol, such as high H/C ratio, the liquid nature at atmospheric pressure, and an industrial scale production from various feedstocks.¹ However, it is still a challenge to apply MSR in fuel cells for efficient production of hydrogen because the by-product, CO, is poisonous to the anode of the cells.^{2, 3} In recent years, massive endeavors have been devoted to improving the activity

and selectivity of catalysts for MSR towards CO₂ and H₂, which can basically be divided into two main groups: copper-based and group 8–10 metal-based catalysts.^{1, 4, 5} Among them, ZnO-supported Cu catalysts are widely used in commerce,^{6, 7} but they suffer from severe coking and sintering at relatively low temperatures.^{5, 8} In contrast, Pd/ZnO catalysts first reported by Iwasa et al.⁹⁻¹² are more efficient for MSR, which combine the advantages of thermal stability and catalytic selectivity. The catalytic functions of Pd/ZnO are greatly improved by the formation of PdZn alloys, which are identified as the real active phase for MSR reactions.^{10, 13, 14} The surface termination and reactivity of PdZn alloys are of great interest. In the investigation of alloying thin Zn layer on Pd(111), a p(2 × 1) LEED pattern was observed at a Zn coverage of 0.5 ML, suggesting an ordered surface termination with a Pd: Zn ratio of 1: 1.¹⁵⁻¹⁷ A theoretical work by Neyman et al. reported that this surface termination is stable because the surface segregation of neither Pd nor Zn is favorable.¹⁸ On the other hand, some studies reported that the geometric structure of the PdZn surface would be rearranged in certain conditions.¹⁹⁻²¹ When exploring the reactivity of PdZn alloys, amount of DFT calculations have been implemented on simplified catalyst models, ranging from the most stable (111) and (100) surface to the defect surface^{17, 22-24} and PdZn nanoparticles²⁵, providing mechanistic understanding of MSR process. Except for PdZn alloys, the ZnO support or ZnO patches formed by partial oxidation of PdZn particles under MSR conditions might also be responsible for the high selectivity.²⁶⁻²⁸

Although MSR is a well-established process experimentally, the reaction mechanisms of MSR are still not fully understood. Based on previous studies,^{22, 24, 29-37} plausible reaction pathways on PdZn and Cu have been reported as follows (R1–R8), where an asterisk (*) represents the adsorbed state.



The above pathway undergoes several key intermediates, e.g., methoxyl (CH_3O^*), formaldehyde (HCHO^*), hydroxymethoxy (H_2COOH^*), formic acid (HCOOH^*) and formate (HCOO^*). It is worth pointing out that the fourth step ($\text{R4: HCHO}^* + \text{OH}^* \rightarrow \text{H}_2\text{COOH}^*$) is critical for MSR because the combination of HCHO^* with OH^* largely suppresses the decomposition of HCHO^* into CO^* and H_2 (the side reaction)³⁸ and thus alleviates the poisoning of the fuel cell anodes. In addition, the reaction of HCHO^* with CH_3O^* to produce $\text{CH}_2\text{OOCH}_3^*$ is another pathway to hinder the decomposition of HCHO^* , but it is unfavorable in the presence of water.^{32,39} The hydroxyl (OH^*) consumed in R4 originates from the decomposition of water (R1). Therefore, water, by supplying hydroxyl, plays an important role in enhancing the selectivity of MSR towards CO_2 and H_2 . What further intrigues us is whether water has other effects in MSR except serving as a reservoir of hydroxyl? This is also the focal point of our work.

In general, water is regarded as no more than solvent or reactant in chemical reactions. However, with the advances in experimental and theoretical techniques, an increasing number of studies were carried out to explore other possible roles of water in atomic-scale. Among them, the catalytic role of water has attracted particular attention. For example, in the gas-phase reactions, water acting as a catalyst notably accelerates the hydrogen-transfer from aldehyde, sulfuric acid, or nitric acid to hydroxyl.⁴⁰⁻⁴³ In aqueous solution, water is found to facilitate the cleavage of C–H, O–H and C–X ($\text{X} = \text{Cl}, \text{Br}$) bonds by constructing hydrogen-bonded complexes.⁴⁴⁻⁴⁷ In heterogeneous catalysis, such as gold-catalyzed CO oxidation,⁴⁸⁻⁵³ propene epoxidation,^{54,55} and others,⁵⁶⁻⁵⁸ a small quantity of water can significantly promote the reaction rates. Similar effect of water is also reported in Pt-^{59,60}, Pd-⁶¹, Ag-^{49,62}, Cu-^{63,64}, TiO_2 -⁶⁵, FeO -⁶⁶ and $\text{Mn}_{0.75}\text{Co}_{0.25}\text{O}_4$ -catalyzed⁶⁷ systems. For MSR-related steps, Maria Flytzani-Stephanopoulos et al.⁶³ reported the promotional role of water in the conversion of methanol to formaldehyde on Cu(111) surface. Wang et al.⁶⁸ theoretically explored the water effect in HCOOH decomposition on Pd(111) and revealed that co-adsorbed H_2O and its coverage could influence this process. Furthermore, Chen et al.⁶⁹ found that the water aggregation could reduce the barrier of water dissociation on PdZn(111). In the reverse reaction, methanol synthesis from CO_2 and H_2 , the catalytic role of water was also reported.^{64,70,71}

While some work studied the water effect on some steps of MSR, an overall picture that describes the catalytic role of water in MSR is still lacking, especially on the Pd/ZnO catalysts. In this article, we present a comprehensive theoretical study of the effect of water in the whole

MSR process from thermodynamics and kinetics. We show that water not only affects the adsorption of reaction species but also the kinetics of the elementary steps of MSR. In the presence of co-adsorbed water, the adsorption energies of reaction species including CH_3OH^* , CH_3O^* , H_2COOH^* , HCOOH^* and HCOO^* are increased by some 0.1–0.3 eV (in absolute value) owing to the hydrogen bonding interactions. Of great importance is that finding that water has a substantial effect in the dehydrogenation steps of MSR, the activation barriers of which are reduced by 0.25–0.46 eV with respect to the cases without co-adsorbed water. Depending on how water participates in the reactions, we classify the catalytic mechanisms of water into two categories, the solvation effect and the H-transfer effect. Therefore, this study maps out an overall picture for the function of water in MSR.

2. Computational details

All self-consistent periodic DFT calculations were performed using DMol³ software as implemented in the Materials Studio package.^{72, 73} The generalized gradient approximation (GGA)⁷⁴ in the form of the PW91 exchange-correlation functional and double-numerical quality basis set with polarization functions (DNP) were employed. The core electrons of metal atoms were treated using effective core potential (ECP).^{75, 76} A thermal smearing of 0.002 hartree and a real-space cutoff of 4.5 Å were adopted.

As the catalytic performance of Pd/ZnO is ascribed to the PdZn alloys,^{13, 14} all the calculations were carried out on the most regular (111) surface of the PdZn alloys.^{77, 78} The lattice parameters of the bulk PdZn crystal, $a = b = 4.11$ Å, $c = 3.35$ Å, were taken from the experimental work.⁷⁸ PdZn(111) was modeled by a periodic four-layer slab repeated in a 4×4 surface unit cell with a 12 Å vacuum slab to separate the periodically repeated slabs (Fig. 1). The bottom two layers were constrained at the bulk position and the top two layers with the adsorbates were allowed to relax. The Brillouin-zone integrations were performed using $3 \times 3 \times 1$ k -point grid. A complete LST/QST (linear synchronous transit and quadratic synchronous transit) approach^{79, 80} and a mode-eigenvector following method⁸⁰ were chosen to determine the transition state structure.

The adsorption energy, E_{ads} , was calculated as follows:

$$E_{\text{ads}} = E_{\text{adsorbate} + \text{surface}} - (E_{\text{adsorbate}} + E_{\text{surface}})$$

where $E_{\text{adsorbate} + \text{surface}}$ is the total energy of PdZn(111) covered with adsorbates, $E_{\text{adsorbate}}$ is the energy of free adsorbate, E_{surface} is the energy of clean PdZn(111) surface. With these definitions,

the more negative the value of E_{ads} is, the more stable the adsorption on the surface will be. All the calculated energies reported herein do not include ZPE-correction.

3. Results and discussion

3.1 Adsorption of key reaction species on PdZn(111)

Before addressing the MSR reactions, we first investigate the adsorption of key reaction species involved in MSR on the PdZn(111) surface. Table 1 lists the adsorption sites, adsorption energies and major structural parameters of key species on PdZn(111) in the absence of water. Calculation results show that species adsorbed via H or C atom prefer sites with more Pd atoms, while species adsorbed via O atom favor sites with more Zn atoms, which is also supported by previous studies.^{29, 32} In theory, the hydrogen and carbon atoms poor in electrons favor the alkalic Pd sites and the oxygen atom rich in electrons prefers the acidic Zn sites. The saturated species, like H_2O^* , HCHO^* and HCOOH^* tend to be adsorbed on top sites, whereas the unsaturated species, like H^* , OH^* , CH_3O^* , H_2COOH^* and HCOO^* favor the bridge or hollow sites. The adsorption energies of unsaturated species are much higher (in absolute value) than those of saturated species as shown in Table 1. In addition, the binding of HCOO^* on the PdZn(111) surface has two possible modes, i.e., bidentate ($bi\text{-HCOO}^*$) and monodenate ($mono\text{-HCOO}^*$), which have the adsorption energy of -2.73 eV and -2.24 eV (bridge adsorption), respectively. Though the bidentate HCOO^* is more stable than monodenate HCOO^* on the surface, the H atom of $bi\text{-HCOO}^*$ points to the gas phase rather than the substrate surface, suggesting the dehydrogenation of $bi\text{-HCOO}^*$ might be difficult to occur.

Table 2 lists the adsorption details of several key species on PdZn(111) in the presence of co-adsorbed water. Compared to the cases without co-adsorbed water, the adsorption geometries of key species change slightly except for methoxyl (CH_3O^*), i.e., CH_3O^* alone preferentially adsorbs at the 3-fold hollow site, $H^{\text{PdZn}2}$, whereas it moves to the 2-fold site, B^{PdZn} , after the introduction of water. As displayed in Table 2, most of the selected species and water could co-adsorb at the neighboring sites of PdZn(111), with calculated adsorption energies falling between -0.89 eV and -3.33 eV. It is interesting to note that the co-adsorption energies of $\text{H}_2\text{O}\cdots\text{H}_2\text{O}^*$, $\text{CH}_3\text{OH}\cdots\text{H}_2\text{O}^*$, $\text{H}_2\text{COOH}\cdots\text{H}_2\text{O}^*$, $bi\text{-HCOO}\cdots\text{H}_2\text{O}^*$ and $mono\text{-HCOO}\cdots\text{H}_2\text{O}^*$ are ~ 0.3 eV (in absolute value) higher than the sum of separated adsorption energies (Table S1), which mainly attributes to the hydrogen bonding interactions between the key species and co-adsorbed water.

As shown in Table S1, the lengths of the hydrogen bonds between water and key species are measured at 1.5–1.8 Å, falling in the typical region for a hydrogen bonding interaction. Based on the above analysis, one can conclude that the introduction of water can enhance the adsorption of key species on PdZn(111).

3.2 Kinetics of MSR with and without co-adsorbed water on PdZn(111)

As mentioned before, the whole MSR process consists of eight elementary steps, including six dehydrogenation steps (the dehydrogenation of H_2O^* , CH_3OH^* and HCOOH^* involving O–H bond cleavage, and the dehydrogenation of CH_3O^* , H_2COOH^* , and HCOO^* involving C–H bond cleavage), the formation of H_2COOH^* , and the generation of H_2 . In the following, the possible catalytic role of water in each step will be discussed in detail.

3.2.1 $\text{H}_2\text{O}^* \rightarrow \text{OH}^* + \text{H}^*$

As shown in Fig. 2, the dissociation of a single water starts from the initial state (IS1-1) with H_2O^* sitting at the Zn top site to the final state (FS1-1) with OH^* and H^* anchored at hollow sites. The activation barrier and reaction energy are calculated to be 1.18 eV and 0.22 eV respectively, in good agreement with the previously reported activation barrier of 1.15 eV and reaction energy of 0.22 eV.⁶⁹ In the presence of a co-adsorbed water, the dissociation of water has two alternative pathways. In the first pathway (IS1-2 \rightarrow TS1-2 \rightarrow FS1-2), the dissociation process only occurs in $\text{H}_2\text{O}(\text{a})^*$, while $\text{H}_2\text{O}(\text{b})^*$ merely serves as a by-stander without involving in $\text{H}_2\text{O}(\text{a})^*$ dissociation. In the second pathway (IS1-3 \rightarrow TS1-3 \rightarrow FS1-3), the two water molecules, $\text{H}_2\text{O}(\text{a}')^*$ and $\text{H}_2\text{O}(\text{b}')^*$, both participate in the dissociation process following an SN_2 -like mechanism: while a hydrogen of $\text{H}_2\text{O}(\text{b}')^*$ transfers to $\text{H}_2\text{O}(\text{a}')^*$, a hydrogen of $\text{H}_2\text{O}(\text{a}')^*$ is simultaneously abstracted to the surface, resulting in the final species H^* , OH^* , and $\text{H}_2\text{O}(\text{a}')^*$. The overall reaction can be expressed as $\text{H}_2\text{O}(\text{b}') \cdots \text{H}_2\text{O}(\text{a}')^* \rightarrow \text{OH}^* + \text{H}_2\text{O}(\text{a}')^* + \text{H}^*$, where $\text{H}_2\text{O}(\text{a}')^*$ is not consumed in the whole reaction but just acts as a mediator for transferring hydrogen atom. Coincidentally, the two pathways possess the same energy profile albeit different structures of transition states and final states. The activation barriers and the reaction energies are 0.92 eV and 0.32 eV, respectively. The dissociation barrier of water dimer is reduced by 0.26 eV with respect to that of single-water dissociation, indicating water itself plays a promotional role in its dissociation.

3.2.2 $\text{CH}_3\text{OH}^* \rightarrow \text{CH}_3\text{O}^* + \text{H}^*$

Although the dissociation of methanol might be initiated by the breaking of O–H, C–O or C–H bonds, previous calculations show that the O–H bond scission is the dominant pathway.²⁴ As shown in Fig. 3, a single CH_3OH^* at Zn top site (IS2-1) dissociates into adsorbed CH_3O^* and H^* with an activation barrier of 1.27 eV and a reaction energy of 0.15 eV, which are close to the previously reported activation barrier of 1.08 eV and reaction energy of 0.28 eV.⁸¹ Analogous to water dissociation, the dehydrogenation of methanol in the presence of co-adsorbed water also has two possible pathways. In the first pathway (red curve in Fig. 3), the dehydrogenation only occurs in methanol, with water serving as a by-stander. The activation barrier and reaction energy are 0.86 eV and 0.29 eV, respectively. Although water does not participate in the dehydrogenation, it does play a critical role in weakening the O–H bond of methanol through hydrogen bonding interaction. In the second pathway (blue curve in Fig. 3), a H-transfer process takes place between water and methanol, i.e., a hydrogen of methanol transfers to water and simultaneously a hydrogen of water is abstracted to the surface. The overall reaction can be expressed as $\text{CH}_3\text{OH}\cdots\text{H}_2\text{O}^* \rightarrow \text{CH}_3\text{O}^* + \text{H}_2\text{O}^* + \text{H}^*$. The activation barrier and reaction energy are calculated to be 0.93 eV and 0.35 eV, respectively. For the two pathways, water is not consumed and just acts as a catalytic promoter, resulting in the reduction of the activation barrier by ~ 0.40 eV with respect to the case without co-adsorbed water.

3.2.3 $\text{CH}_3\text{O}^* \rightarrow \text{HCHO}^* + \text{H}^*$

The dehydrogenation of CH_3O^* to HCHO^* on PdZn(111) is considered to be the rate-limiting step of MSR in previous studies.^{23, 29, 82} As shown in Fig. 4 (black curve), CH_3O^* alone is strongly adsorbed at the 3-fold hollow site, $H^{\text{PdZn}2}$, with an adsorption energy of -2.32 eV. The subsequent dissociation of CH_3O^* to HCHO^* and H^* needs to overcome a barrier of 1.41 eV, which is 0.24 eV higher than the previously reported value.²⁹ Both the high activation barrier and the endothermic reaction energy (1.18 eV) indicate that the dehydrogenation of CH_3O^* is difficult to occur. In the presence of co-adsorbed water, H_2O^* and CH_3O can form a $\text{CH}_3\text{O}\cdots\text{H}_2\text{O}^*$ complex via hydrogen bonding interaction, which results in the barrier of CH_3O^* dehydrogenation being reduced by 0.25 eV. Compared with the dehydrogenation of water and methanol, the catalytic effects of water in this step is a little weaker. Thermodynamically, water favors this step by a decreased reaction energy of 0.58 eV with respect to the path without co-

adsorbed water. As water is unable to form hydrogen bonding with the hydrogen atom of C–H bond, therefore the role of water serving as a H-transfer mediator is not available here.

3.2.4 $\text{HCHO}^* + \text{OH}^* \rightarrow \text{H}_2\text{COOH}^* \rightarrow \text{HCOOH}^* + \text{H}^*$

The reaction between HCHO^* and OH^* to produce H_2COOH^* is a critical step in determining the selectivity of MSR. Our calculation results show that this step is favorable in both kinetics and thermodynamics, with an activation barrier of 0.16 eV and an exothermic reaction energy of 0.48 eV. Previous DFT calculations also gave a similar results of an activation barrier of 0.17 eV and a reaction energy of -0.50 eV.³³ Considering this step could readily occur we thus did not explore the effect of water in this step.

As stated in the introduction section, the decomposition of HCHO to produce CO is the side reaction in MSR process. Then, how water affects this pathway is also worth noting. The decomposition of HCHO experiences two elementary steps, i.e., $\text{HCHO}^* \rightarrow \text{HCO}^* + \text{H}^*$ and $\text{HCO}^* \rightarrow \text{CO}^* + \text{H}^*$. Because the first step ($\text{HCHO}^* \rightarrow \text{HCO}^* + \text{H}^*$) was found to be rate-limiting³⁷, we thus only studied the effect of water in this step. As shown in Table S3, with the assistance of water the activation barrier is still above 0.80 eV, much higher than that of $\text{HCHO}^* + \text{OH}^* \rightarrow \text{H}_2\text{COOH}^*$. Therefore, the reaction of HCHO^* with OH^* remains predominant even though the effect of water on the side reaction is considered.

Fig. 5 (black curve) shows that the dehydrogenation of single H_2COOH^* has an activation barrier of 1.08 eV and a reaction energy of -0.43 eV. While in the presence of co-adsorbed water, the activation barrier is dramatically reduced to 0.62 eV and the reaction energy changes to -0.49 eV. The introduction of water reduces the activation barrier of H_2COOH^* dehydrogenation by 0.46 eV, indicative of the catalytic effects of water. Similar to CH_3O^* , water is unable to construct hydrogen bonding interaction with the C–H bond of H_2COOH^* , thus the role of water serving as a H-transfer mediator is not available either.

3.2.5 $\text{HCOOH}^* \rightarrow \text{HCOO}^* + \text{H}^*$

In the dehydrogenation of formic acid, *trans*- HCOOH^* and *cis*- HCOOH^* are both considered. Our calculation results show that *trans*- HCOOH^* is more stable than *cis*- HCOOH^* both in gas phase and on PdZn(111), suggesting that *trans*- HCOOH^* is probably the dominant species. For the case without co-adsorbed water (black curve in Fig. 6), the dehydrogenation of *trans*- HCOOH^* to HCOO^* is exothermic, with a reaction energy of -0.13 eV and an activation barrier

of 0.71 eV. In the presence of co-adsorbed water, the reaction energy and activation barrier reduce to -0.27 eV and 0.46 eV, respectively, as shown by the red curve of Fig. 6. Note that the hydrogen bonding in IS6-2 is constructed between the H atom of water and the carbonyl oxygen of *trans*-HCOOH*. Theoretically, the H atom of water can also interact with the hydroxyl oxygen of HCOOH*, but the optimized structure is found less stable than IS6-2 and thus is not studied. In the presence of water, the dehydrogenation of HCOOH* starts from *cis*-HCOOH*. As depicted by the blue curve of Fig. 6, *cis*-HCOOH* and water form a weakly hydrogen-bonded complex (IS6-3) with a co-adsorption energy of -0.69 eV. Subsequently, the H-transfer occurs between the *cis*-HCOOH \cdots H₂O* complex and the substrate, leading to the production of adsorbed H*, H₂O* and HCOO*. Water in this process is not consumed and just serves as a mediator for H-transfer. As the water molecule in IS6-3 is pretty far from the substrate surface, ~ 3.5 Å, thus the dehydrogenation barrier is calculated to be 0.67 eV, slightly lower than that of the case without co-adsorbed water. In comparison of the three pathways, we find that the dehydrogenation of *trans*-HCOOH* with a co-adsorbed water is the most favorable to occur, with an activation barrier of 0.46 eV and energy release of 0.27 eV.

3.2.6 $\text{HCOO}^* \rightarrow \text{CO}_2(\text{g}) + \text{H}^*$

As stated above, although the bidentate adsorption of HCOO* is more stable than monodentate adsorption mode, the dissociation of *bi*-HCOO* is predicted difficult to occur since the H atom of *bi*-HCOO* points to gas phase rather than the substrate surface. Recent studies revealed that the dehydrogenation of HCOO* experiences a *bi*-HCOO* \rightarrow *mono*-HCOO* \rightarrow CO₂(g) pathway.^{33, 68} Our calculation results show that the transformation of *bi*-HCOO* to *mono*-HCOO* needs to overcome a high barrier of 0.85 eV, as depicted by the black curve of Fig. 7. However, the subsequent C–H bond cleavage of *mono*-HCOO* is favorable in both kinetics and thermodynamics with an activation barrier of only 0.21 eV and a reaction energy of -0.64 eV. The whole pathway (*bi*-HCOO* \rightarrow *mono*-HCOO* \rightarrow CO₂(g)) is almost thermoneutral with a total reaction energy of -0.05 eV. Therefore, the transformation of *bi*-HCOO* to *mono*-HCOO* is the rate-limiting step in HCOO decomposition. The CO₂ molecule prefers to desorb into gas-phase as soon as it is generated.

In the presence of co-adsorbed water, the transformation barrier from *bi*-HCOO* to *mono*-HCOO* is reduced to 0.54 eV, which is 0.31 eV lower than that of the case without co-adsorbed water. However, the barrier of *mono*-HCOO* dehydrogenation increases by 0.21 eV with respect

to the path without co-adsorbed water, in part because the hydrogen bonding in between H_2O^* and *mono*- HCOO^* breaks as the C–H bond cleaves in TS7-2. In comparison of the structures of IS7-1* and IS7-2*, we find that the introduction of water elongates the distance of the H atom of *mono*- HCOO^* to the substrate surface, from 1.98 Å in IS7-1* to 3.00 Å in IS7-2*, which is another causal reason for the increased dehydrogenation barrier. While water to some degree hinders dehydrogenation of *mono*- HCOO^* , it reduces the barrier of the rate-limiting step (the transformation of *bi*- HCOO^* to *mono*- HCOO^*) from 0.85 eV of the case without co-adsorbed water to 0.54 eV, indicating water still plays a promotional role in the dehydrogenation of HCOO^* .

3.2.7 $\text{H}^* + \text{H}^* \rightarrow \text{H}_2(\text{g})$

The generation of H_2 from adsorbed H atoms is the final step of MSR. Our calculation results show that the combination of two H atoms anchored at two neighboring hollow sites is exothermic by 0.39 eV, with a low barrier of 0.12 eV, as shown in Fig. 8. Similar to CO_2 molecule, H_2 tends to desorb into the gas-phase once it is produced. Considering the easiness of the generation of H_2 , the catalytic effects of water thus is not explored here.

3.2.8 Overview of the catalytic effects of water in MSR

In the sections above, we have systemically studied the catalytic role of water in the whole MSR process except for two low-barrier steps, $\text{HCHO}^* + \text{OH}^* \rightarrow \text{H}_2\text{COOH}^*$ and $\text{H}^* + \text{H}^* \rightarrow \text{H}_2(\text{g})$. For the other six dehydrogenation steps, the introduction of water is found to notably reduce the activation barriers by 0.25–0.46 eV. The catalytic mechanisms of water can be roughly divided into two categories: (i) the solvation effect, which means water only serves as a by-stander to affect the reactions without participating in the bond cleavage and formation, as depicted by Fig. 9(a), and (ii) H-transfer effect, which means water does participate in the H-transfer process but only serves as a mediator to transfer H atom from reactants to the surface, as depicted by Fig. 9(b). In essence, both of the two catalytic mechanisms are based on the hydrogen bonding interaction between water and adjacent species. Remind that the six dehydrogenation steps studied above consist of two groups, O–H bond cleavage and C–H bond cleavage. For the dehydrogenation steps involving O–H bond cleavage, both of the two catalytic mechanisms of water (Fig. 9) are applicable and show a slight difference in reducing the reaction barriers. However, for the dehydrogenation steps involving C–H bond cleavage, water can only

promote reactions through the solvation effect instead of serving as a mediator for H-transfer, mainly because water is unable to construct hydrogen bond with weakly polarized C–H bond.

Considering the computational model with one co-adsorbed water per unit cell might fail to account for the high water coverage in experiment, we re-investigated two high-barrier elementary steps, $\text{CH}_3\text{OH}^* \rightarrow \text{CH}_3\text{O}^* + \text{H}^*$ and $\text{CH}_3\text{O}^* \rightarrow \text{HCHO}^* + \text{H}^*$ by adding two and three water molecules in the unit cell. The calculation results are listed in Table S2. It is shown that both two and three water molecules in one unit cell are also able to reduce the activation barriers of the two steps compared to the cases without co-adsorbed water. Moreover, the variations of activation barrier in the presence of one, two, and three water molecule(s) are within 0.20 eV for the two steps, indicating the slight increase of water coverage will not notably affect the catalytic function of water. On the other hand, if the coverage of water is further increased, resulting in most catalytic centers being occupied, water will surely play a retarding role in the reaction. Overall, understanding the effect of water coverage on the elementary steps is not easy and needs continuous studies.

4. Conclusions

We have systematically investigated the catalytic effects of water in the whole methanol steam reforming (MSR) process using the first-principles calculations. The main conclusions are drawn as follows. First, water is found to play an enhancing role in the adsorption of key species involved in MSR. The co-adsorption of water and reaction species such as CH_3OH^* , CH_3O^* , H_2COOH^* , HCOOH^* and HCOO^* are some 0.10~0.30 eV more stable than separated adsorption, owing to the hydrogen bonding interaction. Second, the introduction of water could notably affect the kinetics of elementary steps of MSR. For six critical dehydrogenation steps, including the rate-limiting step, water is capable of reducing the activation barriers by 0.25–0.46 eV without being consumed, indicating that water does play a catalytic role in MSR. Third, the catalytic mechanisms of water can be roughly divided into two categories depending on how water participates in the reaction: the solvation effect and the H-transfer effect. Both of the two effects are proved effective in the steps that involving O–H bond cleavage, while only the solvation effect is applicable in the steps involving C–H bond cleavage. The interpretation of the catalytic role of water in MSR would provide deeper insights into the reaction mechanisms of MSR and stimulate the interests in exploring the catalytic role of water in other chemical reactions.

***Corresponding author**

Email: changcr@mail.xjtu.edu.cn

Acknowledgements

The authors thank Prof. Jun Li at Tsinghua University for discussion and helping us get access to the software of Materials Studio. This work was supported by the China Postdoctoral Science Foundation (2014M562391), and the Fundamental Research Funds for the Central Universities. The calculations were performed by using supercomputers at Chinese Academy of Sciences and the Shanghai Supercomputing Center.

References

- 1 D. R. Palo, R. A. Dagle and J. D. Holladay, *Chem. Rev.*, 2007, **107**, 3992-4021.
- 2 E. Martono and J. M. Vohs, *J. Phys. Chem. C*, 2013, **117**, 6692-6701.
- 3 G. J. K. Acres, J. C. Frost, G. A. Hards, R. J. Potter, T. R. Ralph, D. Thompsett, G. T. Burstein and G. J. Hutchings, *Catal. Today*, 1997, **38**, 393-400.
- 4 S. Sá, H. Silva, L. Brandão, J. M. Sousa and A. Mendes, *Appl. Catal. B: Environ.*, 2010, **99**, 43-57.
- 5 N. Takezawa and N. Iwasa, *Catal. Today*, 1997, **36**, 45-56.
- 6 D. L. Trimm and Z. I. Önsan, *Catal. Rev.*, 2001, **43**, 31-84.
- 7 S. Fukahori, T. Kitaoka, A. Tomoda, R. Suzuki and H. Wariishi, *Appl. Catal. A: Gen.*, 2006, **300**, 155-161.
- 8 E. Jerero and J. M. Vohs, *J. Am. Chem. Soc.*, 2008, **130**, 10199-10207.
- 9 N. Iwasa, S. Kudo, H. Takahashi, S. Masuda and N. Takezawa, *Catal. Lett.*, 1993, **19**, 211-216.
- 10 N. Iwasa, S. Masuda, N. Ogawa and N. Takezawa, *Appl. Catal. A: Gen.*, 1995, **125**, 145-157.
- 11 N. Iwasa, T. Mayanagi, W. Nomura, M. Arai and N. Takezawa, *Appl. Catal. A: Gen.*, 2003, **248**, 153-160.
- 12 N. Iwasa, T. Mayanagi, S. Masuda and N. Takezawa, *React. Kinet. Catal. Lett.*, 2000, **69**, 355-360.

- 13 Y. H. Chin, R. Dagle, J. Hu, A. C. Dohnalkova and Y. Wang, *Catal. Today*, 2002, **77**, 79-88.
- 14 M. Armbrüster, M. Behrens, K. Föttinger, M. Friedrich, É. Gaudry, S. K. Matam and H. R. Sharma, *Catal. Rev.*, 2013, **55**, 289-367.
- 15 E. Jeroro, V. Lebarbier, A. Datye, Y. Wang and J. M. Vohs, *Surf. Sci.*, 2007, **601**, 5546-5554.
- 16 A. Bayer, K. Flechtner, R. Denecke, H. P. Steinrück, K. M. Neyman and N. Rösch, *Surf. Sci.*, 2006, **600**, 78-94.
- 17 K. M. Neyman, K. H. Lim, Z. X. Chen, L. V. Moskaleva, A. Bayer, A. Reindl, D. Borgmann, R. Denecke, H. P. Steinruck and N. Rosch, *Phys. Chem. Chem. Phys.*, 2007, **9**, 3470-3482.
- 18 Z. X. Chen, K. M. Neyman and N. Rösch, *Surf. Sci.*, 2004, **548**, 291-300.
- 19 C. Weilach, S. M. Kozlov, H. H. Holzapfel, K. Föttinger, K. M. Neyman and G. Rupprechter, *J. Phys. Chem. C*, 2012, **116**, 18768-18778.
- 20 W. Stadlmayr, C. Rameshan, C. Weilach, H. Lorenz, M. Hävecker, R. Blume, T. Rocha, D. Teschner, A. Knop-Gericke, D. Zemlyanov, S. Penner, R. Schlögl, G. Rupprechter, B. Klötzer and N. Memmel, *J. Phys. Chem. C*, 2010, **114**, 10850-10856.
- 21 C. Rameshan, W. Stadlmayr, C. Weilach, S. Penner, H. Lorenz, M. Hävecker, R. Blume, T. Rocha, D. Teschner, A. Knop-Gericke, R. Schlögl, N. Memmel, D. Zemlyanov, G. Rupprechter and B. Klötzer, *Angew. Chem. Int. Ed.*, 2010, **49**, 3224-3227.
- 22 Z. X. Chen, K. H. Lim, K. M. Neyman and N. Rösch, *Phys. Chem. Chem. Phys.*, 2004, **6**, 4499-4504.
- 23 Z. X. Chen, K. H. Lim, K. M. Neyman and N. Rösch, *J. Phys. Chem. B*, 2005, **109**, 4568-4574.
- 24 G. K. Smith, S. Lin, W. Lai, A. Datye, D. Xie and H. Guo, *Surf. Sci.*, 2011, **605**, 750-759.
- 25 K. M. Neyman, R. Sahnoun, C. Inntam, S. Hengrasmee and N. Rösch, *J. Phys. Chem. B*, 2004, **108**, 5424-5430.
- 26 M. Friedrich, S. Penner, M. Heggen and M. Armbrüster, *Angew. Chem.*, 2013, **125**, 4485-4488.
- 27 H. Lorenz, M. Friedrich, M. Armbrüster, B. Klötzer and S. Penner, *J. Catal.*, 2013, **297**, 151-154.

- 28 M. Friedrich, D. Teschner, A. Knop-Gericke and M. Armbrüster, *J. Catal.*, 2012, **285**, 41-47.
- 29 Z. X. Chen, K. M. Neyman, K. H. Lim and N. Rösch, *Langmuir*, 2004, **20**, 8068-8077.
- 30 E. Jerero and J. M. Vohs, *Catal. Lett.*, 2009, **130**, 271-277.
- 31 S. Lin, R. S. Johnson, G. K. Smith, D. Xie and H. Guo, *Phys. Chem. Chem. Phys.*, 2011, **13**, 9622-9631.
- 32 S. Lin, D. Xie and H. Guo, *J. Mol. Catal. A: Chem.*, 2012, **356**, 165-170.
- 33 S. Lin, D. Xie and H. Guo, *J. Phys. Chem. C*, 2011, **115**, 20583-20589.
- 34 X. Li and K. H. Lim, *ChemCatChem*, 2012, **4**, 1311-1320.
- 35 E. S. Ranganathan, S. K. Bej and L. T. Thompson, *Appl. Catal. A: Gen.*, 2005, **289**, 153-162.
- 36 X. K. Gu and W. X. Li, *J. Phys. Chem. C*, 2010, **114**, 21539-21547.
- 37 K. H. Lim, Z. X. Chen, K. M. Neyman and N. Rösch, *J. Phys. Chem. B*, 2006, **110**, 14890-14897.
- 38 Z. Chen, Y. Huang and X. He, *Prog. Chem.*, 2012, **24**, 873-878.
- 39 S. Lin, D. Xie and H. Guo, *ACS Catal.*, 2011, **1**, 1263-1271.
- 40 E. Vöhringer-Martinez, B. Hansmann, H. Hernandez, J. S. Francisco, J. Troe and B. Abel, *Science*, 2007, **315**, 497-501.
- 41 I. Smith, *Science*, 2007, **315**, 470-471.
- 42 B. Long, W. J. Zhang, X. F. Tan, Z. W. Long, Y. B. Wang and D. S. Ren, *J. Phys. Chem. A*, 2011, **115**, 1350-1357.
- 43 J. Gonzalez and J. M. Anglada, *J. Phys. Chem. A*, 2010, **114**, 9151-9162.
- 44 C. Zhao, X. Lin, W. M. Kwok, X. Guan, Y. Du, D. Wang, K. F. Hung and D. L. Phillips, *Chem. Eur. J.*, 2005, **11**, 1093-1108.
- 45 W. M. Kwok, C. Zhao, Y. L. Li, X. Guan, D. Wang and D. L. Phillips, *J. Am. Chem. Soc.*, 2004, **126**, 3119-3131.
- 46 J. Q. Huang, C. S. Yeung, J. Ma, E. R. Gayner and D. L. Phillips, *J. Phys. Chem. A*, 2014, **118**, 1557-1567.
- 47 C. S. Yeung, P. L. Ng, X. Guan and D. L. Phillips, *J. Phys. Chem. A*, 2010, **114**, 4123-4130.

- 48 M. Daté, M. Okumura, S. Tsubota and M. Haruta, *Angew. Chem. Int. Ed.*, 2004, **43**, 2129-2132.
- 49 H. Y. Su, M. M. Yang, X. H. Bao and W. X. Li, *J. Phys. Chem. C*, 2008, **112**, 17303-17310.
- 50 G. M. Mullen, J. Gong, T. Yan, M. Pan and C. B. Mullins, *Top. Catal.*, 2013, **56**, 1499-1511.
- 51 J. Saavedra, H. A. Doan, C. J. Pursell, L. C. Grabow and B. D. Chandler, *Science*, 2014, **345**, 1599-1602.
- 52 R. A. Ojifinni, N. S. Froemming, J. Gong, M. Pan, T. S. Kim, J. M. White, G. Henkelman and C. B. Mullins, *J. Am. Chem. Soc.*, 2008, **130**, 6801-6812.
- 53 L. M. Liu, B. McAllister, H. Q. Ye and P. Hu, *J. Am. Chem. Soc.*, 2006, **128**, 4017-4022.
- 54 M. Ojeda and E. Iglesia, *Chem. Commun.*, 2009, 352-354.
- 55 C. R. Chang, Y. G. Wang and J. Li, *Nano Res.*, 2011, **4**, 131-142.
- 56 B. N. Zope, D. D. Hibbitts, M. Neurock and R. J. Davis, *Science*, 2010, **330**, 74-78.
- 57 Y. Gao and X. C. Zeng, *ACS Catal.*, 2012, **2**, 2614-2621.
- 58 C. R. Chang, X. F. Yang, B. Long and J. Li, *ACS Catal.*, 2013, **3**, 1693-1699.
- 59 X. Q. Gong, P. Hu and R. Raval, *J. Chem. Phys.*, 2003, **119**, 6324-6334.
- 60 S. Chibani, C. Michel, F. Delbecq, C. Pinel and M. Besson, *Catal. Sci. Technol.*, 2013, **3**, 339-350.
- 61 G. Croft and M. J. Fuller, *Nature*, 1977, **269**, 585-586.
- 62 W. S. Sheu and M. W. Chang, *Surf. Sci.*, 2014, **628**, 104-110.
- 63 M. B. Boucher, M. D. Marcinkowski, M. L. Liriano, C. J. Murphy, E. A. Lewis, A. D. Jewell, M. F. G. Mattera, G. Kyriakou, M. Flytzani-Stephanopoulos and E. C. H. Sykes, *ACS Nano*, 2013, **7**, 6181-6187.
- 64 Y. F. Zhao, Y. Yang, C. Mims, C. H. F. Peden, J. Li and D. Mei, *J. Catal.*, 2011, **281**, 199-211.
- 65 K. L. Miller, J. L. Falconer and J. W. Medlin, *J. Catal.*, 2011, **278**, 321-328.
- 66 L. R. Merte, G. Peng, R. Bechstein, F. Rieboldt, C. A. Farberow, L. C. Grabow, W. Kudernatsch, S. Wendt, E. Lægsgaard, M. Mavrikakis and F. Besenbacher, *Science*, 2012, **336**, 889-893.

- 67 Y. Wang, X. Zhu, M. Crocker, B. Chen and C. Shi, *Appl. Catal. B: Environ.*, 2014, **160–161**, 542-551.
- 68 R. Zhang, H. Liu, B. Wang and L. Ling, *J. Phys. Chem. C*, 2012, **116**, 22266-22280.
- 69 Y. Huang and Z. X. Chen, *J. Phys. Chem. C*, 2011, **115**, 18752-18760.
- 70 Y. Yang, C. A. Mims, R. S. Disselkamp, J. H. Kwak, C. H. F. Peden and C. T. Campbell, *J. Phys. Chem. C*, 2010, **114**, 17205-17211.
- 71 Y. Yang, C. A. Mims, D. H. Mei, C. H. F. Peden and C. T. Campbell, *J. Catal.*, 2013, **298**, 10-17.
- 72 B. Delley, *J. Chem. Phys.*, 1990, **92**, 508-517.
- 73 B. Delley, *J. Chem. Phys.*, 2000, **113**, 7756-7764.
- 74 J. P. Perdew, K. Burke and M. Ernzerhof, *Phys. Rev. Lett.*, 1996, **77**, 3865-3868.
- 75 M. Dolg, U. Wedig, H. Stoll and H. Preuss, *J. Chem. Phys.*, 1987, **86**, 866-872.
- 76 A. Bergner, M. Dolg, W. Küchle, H. Stoll and H. Preuß, *Mol. Phys.*, 1993, **80**, 1431-1441.
- 77 Y. Huang and Z. X. Chen, *Langmuir*, 2010, **26**, 10796-10802.
- 78 Z. X. Chen, K. M. Neyman, A. B. Gordienko and N. Rösch, *Phys. Rev. B*, 2003, **68**, 075417.
- 79 T. A. Halgren and W. N. Lipscomb, *Chem. Phys. Lett.*, 1977, **49**, 225-232.
- 80 N. Govind, M. Petersen, G. Fitzgerald, D. King-Smith and J. Andzelm, *Comput. Mater. Sci.*, 2003, **28**, 250-258.
- 81 Y. Huang, X. He and Z. X. Chen, *J. Chem. Phys.*, 2013, **138**, 184701.
- 82 B. A. Peppley, J. C. Amphlett, L. M. Kearns and R. F. Mann, *Appl. Catal. A: Gen.*, 1999, **179**, 31-49.